

## Effect of Pyrene Treatment on the Properties of Graphene/Epoxy Nanocomposites

Soon Cheol Kim, Hyung-il Lee, and Han Mo Jeong\*

Department of Chemistry, University of Ulsan, Ulsan 680-749, Korea

Byung Kyu Kim

Department of Polymer Science and Engineering,  
Pusan National University, Busan 609-735, Korea

Jung Ho Kim and Cheol Min Shin

Research Center, N-Baro Tech Co., Ulsan 689-871, Korea

Received March 17, 2010; Revised May 19, 2010;

Accepted June 13, 2010

### Introduction

Graphene is a two-dimensional nanocarbon that is currently being investigated for applications in a variety of areas.<sup>1</sup> Graphene has unusual properties including a large surface area of  $2,600 \text{ m}^2 \cdot \text{g}^{-1}$ , high thermal conductivity of  $\sim 3,000 \text{ W m}^{-1} \cdot \text{K}^{-1}$ , high electrical conductivity of  $\sim 550 \text{ S} \cdot \text{cm}^{-1}$ , a high modulus of  $\sim 1 \text{ TPa}$ , and a high aspect ratio of several hundreds.<sup>2-4</sup>

Aksay *et al.* recently reported that graphene sheets can be produced in bulk by the thermal expansion of sufficiently oxidized graphite oxide (GO).<sup>5</sup> These exfoliated sheets are called functionalized graphene sheets (FGSs) because some of the oxygen containing groups such as epoxy groups remain after thermal treatment.<sup>6</sup> FGSs have an affinity for polar solvents and polymers,<sup>7-9</sup> as well as have a high electrical conductivity of about  $10 \text{ S} \cdot \text{cm}^{-1}$ .<sup>5</sup>

Polymers such as epoxy resin are generally good electrical insulators. However, an improvement in electric conductivity is necessary for applications that require electrostatic dissipation or electromagnetic radiation shielding.<sup>10</sup> Nanocarbons with high conductivity and a large aspect ratio can be effectively utilized in the preparation of conductive polymer nanocomposites.<sup>11,12</sup> Recent studies have demonstrated the emergence of FGS as fascinating conductive nanofillers with low percolation thresholds.<sup>7-10,12</sup>

In nanocomposites, nanofiller dispersion and interfacial interactions with the matrix polymer can be significantly enhanced through chemical or non-covalent physical modi-

fication of the nanofiller surface character.<sup>13,14</sup> Many researchers have reported that polycyclic aromatic hydrocarbons such as pyrene or perylene are strongly adsorbed onto graphene sheets or carbon nanotubes through  $\pi$ - $\pi$  interactions.<sup>15-17</sup>

We observed that the dispersibility of FGSs in the epoxy resin matrix was improved when the FGSs were treated with pyrene. This paper describes the effect of pyrene treatment on the dispersion, electric, and rheological properties of FGS/epoxy nanocomposites.

### Experimental

**Materials.** Natural graphite (HC-908) with an average particle size of  $8 \mu\text{m}$  was purchased from Hyundai Coma Co., Ltd. (Korea). Bisphenol-A diglycidyl ether (epoxy resin, YD-128) with an epoxy equivalent weight of 184-190 g/equivalent was supplied by Kukdo Chemical Co., Ltd. (Korea). 1,3-Phenylenediamine (Sigma-Aldrich), fuming nitric acid (Matsuno Chemical), potassium chlorate (Kanto Chemical Co., Inc.), and acetone (Daejung Chemicals & Metals Co., Ltd.) were used as received.

**Preparation of FGS.** The graphite oxide (GO) was prepared using the Brodie method.<sup>18</sup> In a typical experiment, a reaction flask with 200 mL fuming nitric acid was cooled to  $0^\circ\text{C}$  in an ice bath, and then 10 g of graphite powder was added to the flask by stirring. Next, 85 g of potassium chlorate was slowly added over 1 h, and the reaction mixture was stirred at  $25^\circ\text{C}$ . After 24 h, the mixture was poured into 3 L of distilled water. The GO was filtered and washed with distilled water until the pH of the filtrate was neutral, dried in a vacuum oven at  $100^\circ\text{C}$ , and then pulverized and screened with a 100 mesh sieve to obtain fine particles. Elemental analysis showed the composition to be  $\text{C}_{10}\text{O}_{3.55}\text{H}_{1.32}$ .

To obtain the FGS, the dried GO was charged in a quartz tube and flushed with nitrogen for 5 min, and then the quartz tube was quickly inserted into a furnace preheated to  $1,100^\circ\text{C}$  and kept in the furnace for 1 min to split the GO into individual sheets through the evolution of  $\text{CO}_2$ .<sup>5</sup> The apparent specific volume of the FGS was  $320 \text{ cm}^3 \cdot \text{g}^{-1}$ , and elemental analysis showed that the composition was  $\text{C}_{10}\text{O}_{0.76}\text{H}_{0.91}$ .

**Preparation of FGS/Epoxy Nanocomposites.** FGSs were dispersed in 100-fold of acetone containing the dissolved pyrene, and the mixture was sonicated at 330 W and 60 Hz for 1 h at room temperature. This dispersion was mixed with epoxy resin and sonicated for 1 h at room temperature. Next, the acetone was evaporated in a drying oven at  $80^\circ\text{C}$  for 12 h and then in a vacuum oven at  $100^\circ$  for 3 h. This mixture was mixed with 14.5 g of hardener, 1,3-phenylenediamine per 100.0 g of epoxy resin, and was outgassed in a vacuum oven at  $100^\circ\text{C}$  for 7 min. This outgassed mixture was poured into a Teflon mold, which was then placed in a drying oven for curing at  $80^\circ$  for 2 h, followed by post-cur-

\*Corresponding Author. E-mail: hmjeong@mail.ulsan.ac.kr

**Table I. Conductivity of FGS/Epoxy Nanocomposite**

Sample	Conductivity (S/cm)
G0P0	$1.81 \times 10^{-13}$
G0P3	$1.40 \times 10^{-13}$
G1P0	$1.92 \times 10^{-13}$
G1P1	$7.43 \times 10^{-13}$
G2P0	$2.54 \times 10^{-13}$
G2P1	$1.45 \times 10^{-11}$
G2P2	$4.44 \times 10^{-7}$
G2P3	$2.24 \times 10^{-7}$
G3P0	$3.07 \times 10^{-6}$
G3P3	$1.59 \times 10^{-5}$
G4P0	$5.16 \times 10^{-6}$
G4P4	$9.67 \times 10^{-5}$

ing at  $150^\circ$  for 2 h. The sample designation codes in Table I refer to the proportions of FGS and pyrene used in the nanocomposites. For example G2P1 contains two parts FGS and one part pyrene per 100 parts epoxy resin and 1,3-phenylenediamine.

**Characterization.** The direct current conductivity across a 0.5 mm thick cast film was measured with a picoammeter (Keithley 237) at room temperature utilizing round silver electrodes measuring  $0.28 \text{ cm}^2$ , which were attached to both surfaces of the specimen. Silver paste was used to ensure good contact between the specimen surface and the electrode.

The morphology of the nanocomposites was examined with a transmission electron microscope (TEM, Hitachi H-8100). To obtain samples for TEM observation, a cast film of the nanocomposite was cryogenically pulverized. Then, the nanocomposite powder was mixed with epoxy resin (EpoFix Resin, Struers) and cured at  $25^\circ\text{C}$  for 24 h. The cured material was microtomed into slices. Images were observed on a 200 mesh copper net with an acceleration voltage of 200 kV.

Dynamic rheological properties were measured with a cone and plate rheometer (Physica, MCR 301) at  $50^\circ\text{C}$  and

15% strain level; the upper limit where the linear viscoelastic behavior was maintained. The cone angle and the diameter of the plate were  $1.0^\circ$  and 25 mm, respectively.

## Results and Discussion

**Electric Conductivity.** Table I shows that the nanocomposite conductivity increases significantly as the unmodified FGS content in the nanocomposite reaches 3 parts per hundred (phr), which suggests that the percolation threshold, where the conductive network becomes interconnected and conductivity distinctly increases,<sup>19,20</sup> is approximately 3 phr. However, the conductivity of G2P2 compared to G2P0 is enhanced about  $10^6$  fold. These results from Table I demonstrate that the dispersion of FGS is enhanced by treatment with pyrene, which causes a reduction in the percolation threshold to about 2 phr.

**Morphology.** Figure 1(a) shows that FGSs are finely dispersed in the matrix of the epoxy resin. Some of the FGS images are blurred due to the very thin nature of the FGS; however, some images are vivid, probably due to a stacked structure. In Figures 1(b) and 1(c), it is evident that the FGS images become more blurred after treatment with pyrene, which suggests that the dispersion of FGS in the epoxy matrix is enhanced by pyrene treatment.

**Rheological Property.** Rheological properties of nanocomposites measured under dynamic oscillatory measurements are sensitively correlated with the nanoscale structures and interfacial interactions.<sup>21</sup> Thus, we examined the rheological properties of the FGS/epoxy nanocomposite in the absence of curing agent.

Figure 2(a) shows a logarithmic plot of the complex viscosity  $\eta^*$  versus angular frequency  $\omega$  measured at  $50^\circ\text{C}$ . Unadulterated epoxy resin (G0P0) exhibits a Newtonian fluid behavior with a nearly constant  $\eta^*$  at an angular frequency less than  $50 \text{ sec}^{-1}$ . This behavior shows that the molecular weights of the epoxy resin are not high enough to cause a shear thinning behavior, which has been observed in polymers with a polydispersity of molecular weights. Figure 2(a) shows that the  $\eta^*$  increases as the FGS content is increased, and this increase is more evident as the amount of pyrene used for the treatment of FGSs is increased. Since

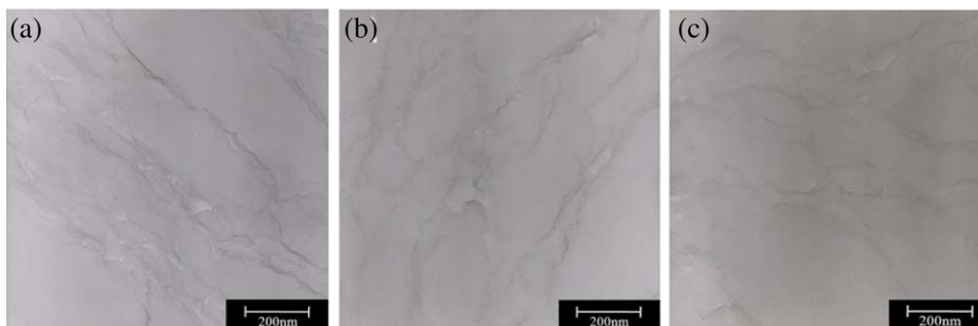


**Figure 1.** TEM micrographs of (a) G2P0, (b) G2P1, and (c) G2P2.

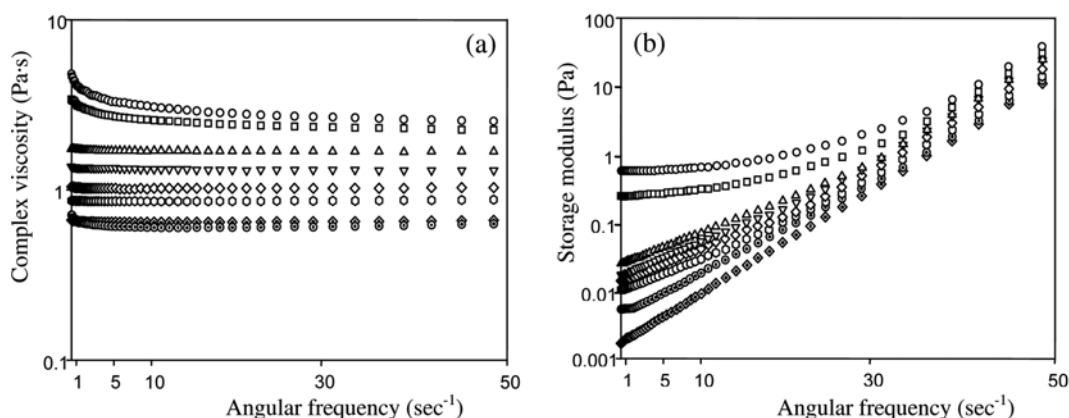


**Figure 2.** (a) Complex viscosity and (b) storage modulus versus angular frequency of (◆) G0P0, (●) G0P3, (◐) G1P0, (◇) G2P0, (▽) G2P1, (△) G2P2, (□) G2P3, and (○) G3P0 containing no 1,3-phenylenediamine.

the  $\eta^*$  of composite increases as the mobility of the matrix material is reduced due to interactions between matrix molecules and filler,<sup>21-23</sup> these results suggest that an increased interfacial area due to a finer dispersion of FGS in the presence of pyrene may be the source of the  $\eta^*$  increase.

The yield behavior, the upturn of  $\eta^*$  at low shear rate (Figure 2(a)) and the diminished frequency dependence of storage modulus at low frequency (Figure 2(b)), becomes evident in G3P0 and G2P3. This yield behavior at low shear rate suggests the possibility of pseudo-solid like behavior that may be attributable to incomplete relaxation.<sup>24,25</sup> Incomplete relaxation of dispersed FGS can be caused by physical congestion of highly anisotropic FGSs, which prevent free rotation in compliance with external dynamic shear. In addition, incomplete relaxation can create a three-dimensional mesoscopic structure for FGSs, not allowing them to independently relax, which in turn cause the observed pseudo-solid like behavior. Thus, the results from Figure 2 suggest that pseudo-solid like behavior is amplified in the presence of pyrene, because pyrene promotes the fine dispersion of FGS in the epoxy resin.

## Conclusions

The results of conductivity, morphology, and complex viscosity experiments demonstrate that dispersion of FGS in epoxy resin can be improved by treatment with pyrene and suggest that pyrene reduces the agglomeration of FGS in epoxy resin. The exact mechanism for this phenomenon requires further study.

**Acknowledgements.** This research was financially supported by the Ministry of Education, Science Technology (MEST) and Korea Institute for Advancement of Technology (KIAT) through the Human Resource Training Project for Regional Innovation. And this work was supported by Priority Research Centers Program through the National

Research Foundation of Korea (NRF) funded by the Ministry of Education, Science and Technology (2009-0093818).

## References

- (1) C. N. R. Rao, A. K. Sood, K. S. Subrahmanyam, and A. Govindaraj, *Angew. Chem. Int. Ed.*, **48**, 7752 (2009).
- (2) G. Wang, X. Shen, B. Wang, J. Yao, and J. Park, *Carbon*, **47**, 1359 (2009).
- (3) X. Wang, L. Zhi, and K. Müllen, *Nano Lett.*, **8**, 323 (2008).
- (4) H. Kim and C. W. Macosko, *Macromolecules*, **41**, 3317 (2008).
- (5) H. C. Schniepp, J.-L. Li, M. J. McAllister, H. Sai, M. Herrera-Alonso, D. H. Adamson, R. K. Prud'homme, R. Car, D. A. Saville, and I. A. Aksay, *J. Phys. Chem. B Lett.*, **110**, 8535 (2006).
- (6) K. N. Kudin, B. Ozbas, H. C. Schniepp, R. K. Prud'homme, I. A. Aksay, and R. Car, *Nano Lett.*, **8**, 36 (2008).
- (7) P. Steurer, R. Wissert, R. Thomann, and R. Mülhaupt, *Macromol. Rapid Commun.*, **30**, 316 (2009).
- (8) A. V. Raghu, Y. R. Lee, H. M. Jeong, and C. M. Shin, *Macromol. Chem. Phys.*, **209**, 2487 (2008).
- (9) H. B. Lee, A. V. Raghu, K. S. Yoon, and H. M. Jeong, *J. Macromol. Sci.-Phys.*, in press.
- (10) S. Barrau, P. Demont, A. Peigney, C. Laurent, and C. Lacabanne, *Macromolecules*, **36**, 5187 (2003).
- (11) P. Chen, H.-S. Kim, and H.-J. Jin, *Macromol. Res.*, **17**, 207 (2009).
- (12) J. Y. Jang, H. M. Jeong, and B. K. Kim, *Macromol. Res.*, **17**, 626 (2009).
- (13) S. Barrau, P. Demont, E. Perez, A. Peigney, C. Laurent, and C. Lacabanne, *Macromolecules*, **36**, 9678 (2003).
- (14) G. Pécastaings, P. Delhaès, A. Derré, H. Saadaoui, F. Carmona, and S. Cui, *J. Nanosci. Nanotechnol.*, **4**, 838 (2004).
- (15) J. Liu, W. Yang, L. Tao, D. Li, C. Boyer, and T. P. Davis, *J. Polym. Sci. Part A: Polym. Chem.*, **48**, 425 (2010).
- (16) T. Tanigaki, H. Nishikiori, S. Kubota, N. Tanaka, M. Endo, and T. Fujii, *Chem. Phys. Lett.*, **448**, 218 (2007).
- (17) W. Yang and H. Grennberg, *ECS Trans.*, **19**, 211 (2009).
- (18) H.-K. Jeong, Y. P. Lee, R. J. W. E. Lahaye, M.-H. Park, K. H.

- An, I. J. Kim, C.-W. Yang, C. Y. Park, R. S. Ruoff, and Y. H. Lee, *J. Am. Chem. Soc.*, **130**, 1362 (2008).
- (19) S.-M. Yuen, C. M. Ma, H.-H. Wu, H.-C. Kuan, W.-J. Chen, S.-H. Liao, C.-W. Hsu, and H.-L. Wu, *J. Appl. Polym. Sci.*, **103**, 1272 (2007).
- (20) J. Li, M. L. Sham, J.-K. Kim, and G. Marom, *Compos. Sci. Technol.*, **67**, 296 (2007).
- (21) S. S. Ray, *J. Ind. Eng. Chem.*, **12**, 811 (2006).
- (22) T. D. Fornes, P. J. Yoon, H. Keskkula, and D. R. Paul, *Polymer*, **42**, 9929 (2001).
- (23) Y. B. Cho, H. M. Jeong, and B. K. Kim, *Macromol. Res.*, **17**, 879 (2009).
- (24) C. D. Han and H.-H. Yang, *J. Appl. Polym. Sci.*, **33**, 1221 (1987).
- (25) L. A. Utracki, *Polym. Eng. Sci.*, **28**, 1401 (1988).